Author Manuscript

Author Manuscript

Author Manuscript

Author Manuscript

HHS Public Access

Author manuscript

J Chromatogr A. Author manuscript; available in PMC 2019 April 13.

Published in final edited form as:

J Chromatogr A. 2018 April 13; 1545: 75–83. doi:10.1016/j.chroma.2018.02.052.

Heparin/Heparan Sulfate Analysis by Covalently Modified Reverse Polarity Capillary Zone Electrophoresis-Mass Spectrometry

Patience Sanderson[a], **Morgan Stickney**[a], **Franklin E. Leach III**[a], **Qiangwei Xia**[b], **Yanlei Yu**[c], **Fuming Zhang**[c], **Robert J Linhardt**[c], and **I. Jonathan Amster**[a,*]

[a]140 Cedar Street, University of Georgia, Athens, GA 30602

[b]760 Parkside Avenue, STE 211, CMP Scientific, Corp., Brooklyn, NY, 11226

[c]Biotech 4005, 110 8th Street, Rensselaer Polytechnic Institute, Troy, NY, 12180

Abstract

Reverse polarity capillary zone electrophoresis coupled to negative ion mode mass spectrometry (CZE-MS) is shown to be an effective and sensitive tool for the analysis of glycosaminoglycan mixtures. Covalent modification of the inner wall of the separation capillary with neutral or cationic reagents produces a stable and durable surface that provides reproducible separations. By combining CZE-MS with a cation-coated capillary and a sheath flow interface, a rapid and reliable method has been developed for the analysis of sulfated oligosaccharides from dp4 to dp12. Several different mixtures have been separated and detected by mass spectrometry. The mixtures were selected to test the capability of this approach to resolve subtle differences in structure, such as sulfation position and epimeric variation of the uronic acid. The system was applied to a complex mixture of heparin/heparan sulfate oligosaccharides varying in chain length from dp3 to dp12 and more than 80 molecular compositions were identified by accurate mass measurement.

Keywords

Capillary zone electrophoresis; Mass spectrometry; Sulfated glycosaminoglycan; Reverse polarity; Covalent capillary coating; Mixture analysis

1. INTRODUCTION

Sulfated glycosaminoglycan (GAG) carbohydrates are linear, acidic polysaccharide chains that are abundant on the surface of mammalian cells [1]. Several biological processes, such as developmental and disease functions, are impacted by GAGs within the body through protein-binding interactions [2–4]. The biosynthesis of GAG chains is a non-template

*Corresponding Author: I. Jonathan Amster, jamster@uga.edu, 140 Cedar Street, University of Georgia, Athens, GA 30602, 706-542-2726.

Publisher's Disclaimer: This is a PDF file of an unedited manuscript that has been accepted for publication. As a service to our customers we are providing this early version of the manuscript. The manuscript will undergo copyediting, typesetting, and review of the resulting proof before it is published in its final citable form. Please note that during the production process errors may be discovered which could affect the content, and all legal disclaimers that apply to the journal pertain.

Author Manuscript Author Manuscript Author Manuscript Author Manuscript

process, facilitated by a number of enzymatic steps (elongation, deacetylation, sulfation, epimerization) that do not go to completion, and results in highly heterogeneous and complex mixtures [5]. There are several classes of GAGs that are defined by their linkage pattern and amino sugar (*N*-acetyl glucosamine (GlcNAc) or*N*-acetyl galactosamine (GalNAc)), with heparin and heparan sulfate as the most structurally diverse. Heparin and heparan sulfate consist of a repeating disaccharide unit of an *N*-acetyl glucosamine linked (1←4) to a hexuronic acid sugar. The GlcNAc can be modified by deacetylation and *N*-sulfo modification, and it can also have sulfation at the 6-*O*- or 3-*O*-position. The hexuronic acid sugar can also exist as one of two epimers: glucuronic acid (GlcA) or iduronic acid (IdoA) with sulfation most likely at the 2-*O*-position of IdoA but infrequently at the 2-*O*-position of GlcA [6].

The structural assignment of GAG chains is a significant analytical challenge and has been the target of several researchers [7–14]. Although full-length sulfated GAGs have been analyzed in top-down fashion by mass spectrometry [15, 16], the typical approach is to partially digest polysaccharides to oligosaccharide mixtures of moderate length (typically disaccharides to decasaccharide) to enable characterization. The structural analysis of sulfated GAGs can be accomplished using mass spectrometry, which has the advantages of high sensitivity and selectivity for structural characterization [10, 12, 13, 17, 18].

The complexity of these digest mixtures makes prior separation (on-line or off-line) desirable to facilitate analysis. Some approaches for separating GAGs include high performance liquid chromatography (HPLC), hydrophilic interaction liquid chromatography (HILIC), and capillary zone electrophoresis (CZE). HPLC is a large umbrella term that contains several different techniques based on the chosen column. Size exclusion (SEC), strong anion exchange (SAX), reversed phase ion pairing (RPIP), and graphitized carbon chromatography (GCC) are techniques that have been coupled to mass spectrometry for GAG analysis [19–22]. However, these techniques have disadvantages in comparison to CZE-MS. SEC and SAX utilize reagent cations at elevated concentrations that lead to ion suppression if not removed before MS analysis [23]. RPIP-LC-MS can lead to mass spectrometer contamination and may undermine system performance. HILIC uses a polar stationary phase and mobile phases much like those used in reverse-phase separations, making it more compatible for GAG separations and MS analysis [24, 25]. Unfortunately, HILIC separations resolve components mostly by their degree of polymerization (dp), and do not provide much resolution for isomers [14, 16]. GCC offers adsorption based separation with very stable graphite columns allowing a multitude of conditions to be implemented, such as high temperatures, variable pH, and low salt content [19, 26, 27]. Previous work using HPLC and HILIC demonstrated the ability to separate GAGs up to dp14 [20, 28].

Because of the ionic nature of sulfated GAG chains, CZE is a well-suited separation technique for this biomolecule class. Anionic biomolecules, such as oligonucleotides and metabolites, have been analyzed using CZE for several years [29–33]. Despite this advantage, CZE-MS analysis of GAG oligosaccharides remains an under-developed approach. Much of the early GAG CZE literature focuses on normal mode polarity where a positive potential is applied to the capillary [34–36]. Using normal polarity, CZE separation

Author Manuscript Author Manuscript Author Manuscript Author Manuscript

of chondroitin sulfate, hyaluronic acid, keratan sulfate, heparan sulfate, and heparin; ranging from disaccharide to oligosaccharide length (up to dp20) has been demonstrated [37]. However, normal polarity is not well suited to the acidic nature of highly sulfated GAGs and generally leads to longer migration times (except with specific electrolytes) and low resolution [35, 36, 38]. Most of this work has been performed with optical detection and structural features cannot be assigned without the use of standards. Replacement of UV-absorbance with MS detection is a logical progression; however, the electrolytes used during UV detection experiments are non-volatile and often incompatible with MS limiting the number of well understood electrolytes that can be employed [39–41].

The optimal CZE-MS configuration for GAG oligosaccharide analysis is reverse polarity with negative mode ionization. In reverse polarity CZE, a negative potential is applied to the capillary inlet, generating an electrophoretic force for negatively charged GAGs in the direction of the mass spectrometer. By using reverse polarity, the migration times of GAGs will decrease and the sample peaks become narrower, improving resolution. A recent application of CZE-MS to GAGs has used reverse polarity CZE and negative mode MS detection [42]. This work focused on disaccharides and demonstrated fast and complete separations. Researchers have started to tackle larger oligosaccharides, which retain structural information, in an attempt to solve specific biological problems [37] and investigate common pharmaceuticals [42].

In addition to the electrophoretic force (EF), ions are also subject to an electroosmotic force (EOF). The EOF is driven by the bulk movement of solvated counterions near the inner surface of the capillary. With a conventional bare fused silica (BFS) capillary, the inner surface of the capillary presents silanol groups to the solution within the capillary. At neutral pH, the silanol groups are ionized, resulting in a negatively charged static layer which attracts cations from the background electrolyte (BGE) to create a positively charged mobile layer [43, 44]. With reverse polarity CZE in a BFS capillary, the EOF opposes the EF and results in longer migration times, or may cause some less ionized components to migrate away from the MS interface and not be detected. Modification of the surface of the fused silica capillary can alter its properties and either turn off EOF by creating a neutral surface or make a static positively-charged surface, which would produce an EOF that moves in the same direction as the EF, thus reduces the migration time of the analytes [45, 46]. Prior work used dynamic coatings to create a static positive charge at the inner surface [47, 48]. These are simple to implement, but the stability of such non-covalent coatings is an issue that can be improved upon.

The present work focuses on the separation and detection of GAG oligosaccharide mixtures using reverse polarity CZE-MS. We have examined neutral and cation coated separation capillaries, using covalent modifications that are durable and stable. These were tested and compared to BFS capillaries to optimize separation parameters for GAGs. Baseline characterization of each coating was performed with binary mixtures of typical modifications in GAGs. The optimized conditions were used to examine a complex mixture of GAG oligosaccharides with up to 12 saccharide subunits. Although demonstrated on a high resolution MS system, the described methodology is amenable to most MS instrumentation.

Author Manuscript Author Manuscript Author Manuscript Author Manuscript

2. MATERIALS AND METHODS

2.1. Materials

BFS capillaries (360 μm o.d. x 50 μm i.d.) were purchased from PolyMicro Technologies (Phoenix, AZ), and coated electrospray emitters (1.0 mm OD x 0.75 mm ID, E-BS-CC1-750-1000-10μ-B30) were obtained from CMP Scientific (Brooklyn, NY). Coating reagents, dichlorodimethylsilane (DMS, Sigma-Aldrich, St. Louis, MO) and N-(6-aminohexyl) aminomethyltriethoxysilane (AHS, Gelest, Morrisville, PA) were prepared in toluene. Ammonium acetate, formic acid, water, and methanol were of HPLC grade (Fisher Scientific, Hampton, NH). Diethylamine, sodium hydroxide, concentrated hydrofluoric acid (~48% wt), acetone, and toluene were purchased from Sigma-Aldrich (St. Louis, MO). All solutions were filtered with 0.45 μm syringe filter (Millipore, Temecula, CA) before use.

2.2. GAG Standards

GAG oligosaccharides were prepared by enzymatic depolymerization and purified using strong anion exchange high-pressure liquid chromatography (SAX-HPLC) for samples 1–6 as shown in Table 1 [49]. Epimer pair heparan sulfate tetrasaccharides (Table 1, samples 7 GlcA-GlcNAc6S-IdoA-GlcNAc6S (GI) and 8 GlcA-GlcNAc6S-GlcA-GlcNAc6S (GG)) were chemically synthesized and purified as described in the literature [50]. Low molecular weight heparin, Enoxaparin, was from the USP (Rockville, MD). All samples were desalted with a 3 kDa Amicon Ultra centrifugal filter (Millipore, Temecula, CA) prior to separation and mass spectrometry analysis. Although the GAGs have molecular weights below 3kDa, heparan sulfate tetrasaccharides and larger chains do not pass through the 3kDa membrane. The membrane permeability is based on size and shape. GAGs have a linear structure compared to proteins that often globular, and this makes the GAGs behave as if they have a higher molecular weight to the centrifugal filter membrane. Filters were conditioned with water, and the sample was then washed with two filter volumes of water (14,000 × g for 25 min each). Before analysis, GAG samples were diluted to 5 μg/mL in water.

2.3. Coatings

Bare fused silica capillaries were etched with concentrated hydrofluoric acid (HF) at one end to reduce the outer diameter of the capillary for use in the sheath flow CE interface described below. For the etching process, the outlet of the capillary was placed in concentrated HF for 45–60 min. The capillary tip was then washed profusely with water. The etched capillaries were coated with AHS to render a cation coated capillary and DMS to generate a neutral coated capillary. Coating solutions were prepared in toluene with 1% concentration of either AHS or DMS. To clean and prepare for coating, the capillary was rinsed with 0.1 M NaOH, water, methanol, dry acetone, and dry toluene, respectively, for 30 min each. The capillary was then coated by flowing 1% AHS or DMS for 1 h. The capillary was consecutively flushed with dry toluene, dry acetone, and methanol for 30 min to remove excess coating solution. Finally, the capillary was equilibrated with background electrolyte buffer (BGE, 25 mM ammonium acetate 70% MeOH) for 1 h. Once degradation becomes apparent, BFS capillaries can be easily cleaned by flushing sodium hydroxide for a short time; however, the coatings are stripped in basic conditions and must be reapplied by

Author Manuscript Author Manuscript Author Manuscript Author Manuscript

repeating the coating procedure. In some experiments, 0.1–1% formic acid (FA) or 0.02–0.1% diethylamine (DEA) was added to the BGE.

2.4. Instrumentation

Experiments were conducted on an Agilent HP 3D capillary electrophoresis instrument (Wilmington, DE). The total length of the capillary ranged from 52–54 cm, and its inner diameter was 50 μm with a volume of approximately 1 μL. The aqueous GAG sample was injected for 3 s at 950 mbar followed by a BGE injection for 10 s at 10 mbar. The injected volume was 0.1 μL. The ionic strength of the injected sample plug is 2–3 orders of magnitude less than that of the background electrolyte, so sample stacking is expected under these conditions and provides a sharp sample front. The capillary was then placed into a BGE vial for separation. A separation voltage of -30 kV was applied to the capillary for most experiments. A separation voltage of −15 kV was used for selected experiments as identified in the results below.

An EMASS-II (CMP Scientific, Brooklyn, NY) CE-MS interface was employed to couple the CE with a Thermo Scientific Velos Orbitrap Elite mass spectrometer (Bremen, Germany) [42, 51, 52]. The etched capillary outlet was nested inside of a cation coated glass emitter tip with a 30 μm tip orifice (CMP Scientific, Brooklyn, NY). The etched capillary was positioned 0.3–0.5 mm from the tip of the emitter orifice to create a mixing volume of ca. 15 nL, and the emitter tip was filled with sheath liquid (SL, 25 mM ammonium acetate 70% MeOH). An external power supply provided a nano-electrospray (nESI) voltage ranging from −1.7 to −1.85 kV to the emitter. MS detection was performed in negative ion mode. Prior to CZE-MS experiments, a semi-automatic optimization of source parameters was performed using sucrose octasulfate to improve sensitivity of sulfated GAGs and reduce sulfate loss during MS analysis. The Orbitrap was scanned from m/z 150–2000 for GAG oligosaccharides with a specified resolution of 120,000. Optimal conditions resulted when the S-lens RF level, multipole 00 offset, and lens 0 were set at 6 %, 7.20 V, and 8.50 V, respectively.

3. RESULTS AND DISCUSSION

3.1. Coatings

In capillary zone electrophoresis of mixtures, EF provides component separation due to differences in their mobilities. In contrast, EOF causes an analyte-independent migration of all components. The magnitude and direction of the EOF with respect to the EF depends upon the chemical nature of the separation capillary’s inner surface. In an uncoated BFS capillary, with a background electrolyte solution (BGE) of 25 mM ammonium acetate (pH=7.5) in 70% methanol, a static layer of negatively-charged silanol groups are presented at the inner wall of the capillary. These interact with the BGE to create a mobile layer of solvated positive ions. With reverse-polarity CZE, this mobile layer is attracted by the negative potential at the entrance of the separation capillary. This creates an EOF that opposes the EF for negatively charged analytes. In the case of highly-charged GAG oligosaccharide anions, the EF is greater than the EOF, so sample migrates toward the mass

Author Manuscript Author Manuscript Author Manuscript Author Manuscript

spectrometer interface. However, with EOF moving in the opposite direction, sample migration through the BFS capillary is slowed and results in increased migration times.

We have examined coated capillaries that eliminate the EOF, or reverse it so that it aligns with the EF to optimize the separation of GAG oligosaccharides. After optimization, migration time and peak widths are reduced while the peak capacity remains the same compared to prior work with BFS capillaries. Two different coatings, dichlorodimethylsilane (DMS) and N-(6-aminohexyl) aminomethyltriethoxysilane (AHS), were examined. Figure 1 compares the direction of EF and EOF for BFS, with that of capillaries with neutral (DMS) and cationic (AHS) coatings that were examined for this study.

For DMS and AHS capillaries, the reagent forms a covalent ether linkage to silica at the surface of the inner wall of the capillary and produces a durable and stable layer. These fused silica surface modifications have been used by others for nanoparticle modification, protein immobilization supports, and other applications [53–55]. Non-covalent coating methods (also known as dynamic coating) are easier to implement than covalent coating, but the coating can dissociate from the inner surface over time. In our hands, when bovine serum albumin (BSA) is utilized as a non-covalent coating, a cation surface is produced on the inner surface of the capillary but is unstable over time and often leads to plug formation within the capillary as the coating degrades. As shown in Figure 2, the covalently linked coatings are more durable than the BSA-coated capillaries. After 81 run iterations on a BSA capillary, degradation of the BSA coating caused plug formation and prevented further trials. The AHS and DMS coated capillaries are found to be quite stable, and the coating hydrolyzes slowly under the separation conditions with a very modest change in migration time from run to run. Furthermore, they do not lead to column plugging, and therefore can be refreshed by reapplication of the coating. In contrast, the BSA coated capillaries often become plugged by desorbed protein after several runs.

With a DMS-coated capillary, silanols are capped by neutral methyl groups. This eliminates the EOF in normal and reverse polarity and analytes migrate only under the influence of EF. For negatively-charged analytes under reverse-polarity conditions, the sample is expected to migrate through the capillary faster than in an uncoated BFS capillary. The AHS coated capillary will have an EOF that aligns with the EF for negatively-charged analytes in reverse-phase CZE and should exhibit even faster migration. Multiple amino silane reagents were considered, such as 3-aminopropyltriethoxysilane and N-(2-aminoethyl)-3-aminopropyltriethoxysilane. However, AHS was shown to be the most stable coating reagent because its chain length prevents hydrolysis by self-cyclization [53]. Short term durability tests demonstrated that covalent coatings are stable in optimized conditions (Figure 2), but long-term use showed signs of degradation in DMS coated capillaries. Both coatings degrade in high pH conditions (pH >12).

3.2. CZE-MS of Tetrasaccharides

Tetrasaccharide standards that contain common variations in GAG structure were used to test the efficacy of the coatings. A mixture of tetrasaccharides that differ in the number of sulfate modifications, ranging from 3 to 6 (samples 1–3), was analyzed first. Figure 3 compares the CZE migration profiles (base peak chromatogram) for this GAG

Author Manuscript Author Manuscript Author Manuscript Author Manuscript

tetrasaccharide mixture obtained with BFS, DMS, and AHS coatings on capillaries of similar length and identical experimental conditions. Sample 1 migrates through all of the capillaries first due to the higher number of sulfates present (six) compared to samples 2 and 3 with four and three sulfates, respectively. As expected from the EOF behavior described above, the compounds migrate most rapidly with the AHS capillary and slowest with a BFS capillary. The peaks are narrowest with the AHS capillary, as longitudinal diffusion of a sample band increases linearly with its migration time. For sample 1, the peak widths at 50% peak height (FWHM) were 1.14, 0.49, and 0.2 min for BFS, DMS, and AHS capillaries, respectively. With a decrease in peak width, the sensitivity (limit of detection of 50 ng/mL) was improved using the AHS capillary and optimized experimental conditions. Shortened migration and reduced peak width were achieved with reverse polarity CZE on a cation coated capillary.

Next, compounds that contain single point variations in structure and produced mixtures of increasing separation difficulty were analyzed. Two GAG tetrasaccharides with different amino modifications, samples 4 and 2 (Table 1), were investigated. These tetrasaccharides have the same number of sulfate modifications, but one has an *N*-sulfo modification on the fourth residue; whereas, the other tetrasaccharide contains an *N*-acetyl group. Using reverse polarity CZE-MS on an AHS capillary, these tetrasaccharides are baseline separated in less than 20 min with approximately 2.5 min between the peaks. The FWHM for the peaks are 13.8 s (sample 4) and 15 s (sample 2). When compared with the DMS and BFS capillaries, the FWHM for the AHS capillary was reduced by a factor of two (DMS) or three (BFS). The two components of this mixture differ in composition by (*O*-sulfo + N-acetyl) versus (OH + *N*-sulfo), evidenced by the 42 Da difference in their mass spectra, shown in panels B and C of Figure 4.

A more challenging test are the isomeric tetrasaccharides, samples 5 and 6. The analyte structures are closely related and vary only in the position of one of the five sulfate modifications. Figure 5 shows the separation of this isomer pair (samples 5 and 6) using an AHS coated capillary, with baseline separation of the peaks. As these are positional isomers, their mass spectra are identical, and exhibit double, triply, and quadruply-charged molecular ions, as shown in the lower panel of Figure 5, for sample 5.

The most challenging analysis that often arises in GAG characterization using MS is the differentiation of stereoisomeric compounds arising from epimerization of uronic acids (GlcA vs. IdoA). We examined such a mixture of epimers, and the results are shown in Figure 6, for samples 7 (GI) and 8 (GG). These GAG tetrasaccharides vary only by the C-5 stereochemistry of the uronic acid near the reducing end. With reverse polarity CZE-MS on an AHS capillary, the two epimers are well separated. The early migrating peak, GI, exhibits a distinct shoulder. A similar result was found using differential ion mobility of these same compounds and was attributed to anomeric nature of the reducing end [56]. The rate of mutarotation of the anomeric carbon is slow compared to the migration time in CZE so this is a plausible cause of the extra peak in the sample. The lower panel in Figure 6 shows the mass spectrum of GI which is identical to that of GG (spectrum not shown). Since these are stereoisomers, all of the peaks in the electropherogram, including the shoulder, produce similar ESI mass spectra.

Author Manuscript Author Manuscript Author Manuscript Author Manuscript

3.3. CZE-MS of Enoxaparin (LMWH)

Enoxaparin, a pharmaceutical product produced by alkaline depolymerization of heparin into low molecular weight components, was also analyzed using reverse polarity CZE and negative ion mode mass spectrometry. Others have analyzed Enoxaparin using on-line separations and mass spectrometry detection [14, 57–60]. This sample is known to be a complex mixture of oligosaccharides varying in degree of polymerization (dp) from dp 3 to dp 20. Figure 7A shows an ESI mass spectrum of the sample without any prior separation, demonstrating the innate complexity of this sample. Base peak electropherograms obtained using BFS, DMS, and AHS capillaries are shown Figure 7B. Enoxaparin migrates more quickly through the capillary on the cation coated capillary (AHS) compared to the neutral and uncoated capillaries.

Although the migration time decreases for the coated capillaries, peaks are not lost. The peaks become narrower when using coated capillaries, as shown previously with the tetrasaccharide mixtures, but they exhibit the same features as the BFS separation. This is a highly complex mixture, and we do not obtain baseline separation of all components. Nevertheless, the mass spectra obtained at any time point is highly simplified compared to the unseparated sample, and we can evaluate the components that are present. Oligosaccharides ranging from dp 3 to dp 12 were detected with a range of 4–17 sulfo groups present on the GAGs. The neutral masses extend from 753 to 3301 Da with less than 3.5 ppm error for the assigned compositions. Shorter oligosaccharides migrate through the capillary first and the GAG chain length increases over the migration period. The majority of the chains were dp 4 to dp 8 which is expected for the Enoxaparin mixture. Toward the end of the separation, dp 10 to dp 12 are observed in low intensity.

Sodium and ammonia adducts were also assigned for approximately half of the compositions. Sodium adducts are expected because Enoxaparin is manufactured as a sodium salt. The appearance of ammonia adducts can be explained by the choice of an ammonium acetate BGE. A supplemental list of all 83 unique compositions that were identified using the AHS capillary is included (Supp. Table 1).

3.4. Additives for Separation

While optimizing conditions for reverse polarity CZE with negative ionization mode MS, the use of background electrolyte solution (BGE) additives was explored. The role of pH can play a vital part in the extent of separation achieved based on the applied coating. EOF is directly influenced by the pH range of the BGE on capillaries that have a charge on the inner surface of the capillary. The neutral DMS capillary will not be affected by the pH of the BGE because the EOF is eliminated.

Formic acid (FA) and diethylamine (DEA) were used to adjust the pH to lower and higher values during separation, respectively. These reagents were selected for their volatility, which makes them compatible with on-line CZE-MS analysis. Acetic acid and formic acid were both tested as an additive to the BGE and sheath liquid. Using formic acid reduced the amount of chemical background in the MS which improved the signal to noise ratio compared to acetic acid. Table 2 shows the effect of different BGE additives on the pH of the

Author Manuscript Author Manuscript Author Manuscript Author Manuscript

BGE. Without any additive, a BGE consisting of 25 mM ammonium acetate in 70% MeOH has a pH of 7.5. By adding FA to a concentration of 0.5%, the pH is reduced to 4.2. Conversely, with addition of 0.4 % DEA into the BGE, the pH increases to 10.1.

For the AHS cation coated capillary, increasing the pH of the BGE reduces ionization of the modified surface of the capillary, reduces EOF, and results in longer migration times. In Figure 8, a mixture of tetrasaccharides containing an increasing number of sulfate groups, ranging from 3 to 6 sulfate groups (samples 1–3, and 6), is separated using 25 mM ammonium acetate in 70% MeOH with the addition of FA in the top electropherogram and DEA in the bottom electropherogram. The middle electropherogram is the separation in normal BGE without any pH adjustment. FA reduces the migration time and suppresses sodium adducts in the mass spectrum but does not affect the observed charge state. It also decreases the peak width in the electropherogram. The FWHM for sample 1 is reduced to 16 s using 0.1% FA compared to a FWHM of 22 s without any additive. In contrast, DEA increases migration times and the charge states of the ions of interest in the mass spectrum. As one would expect, DEA increases the peak width. For samples that migrate slower through the capillary, the peak widths increase. Peak broadening is diminished for samples that migrate faster through the capillary. Comparison of sample 1 with or without DEA, the FWHM slightly increases from 21 to 22 s. However, for sample 2 and 3, the FWHM changed from 30 to 85.2 s and 22 to 28 s with the addition of 0.05% DEA, respectively. Overall, lower pH decreases migration time; while, higher pH increases migration time on an AHS cation coated capillary.

4. CONCLUSIONS

In this work, the advantages of using different coated capillaries with reverse polarity CZE-MS separations were demonstrated on oligosaccharide mixtures larger than disaccharides. Standard uncoated, neutral coated, and cation coated capillaries were investigated to determine suitable CZE-MS conditions for sulfated glycosaminoglycans. Covalently coated capillaries were implemented through simple chemical reactions with silane reagents.

Using a cation coated capillary, structurally similar sulfated GAG oligosaccharides and complex mixtures were separated and analyzed with CZE-MS in a fast and reproducible manner. Positional isomers and stereoisomer tetrasaccharides were baseline separated. Although Enoxaparin was not baseline separated, the mass spectra were significantly simplified and would facilitate tandem mass spectrometry of the various components in this mixture. By incorporating a covalent cation coating, the migration time and peak widths were reduced while increasing the analytically useful lifetime of the separation capillary. Through the use of additives, the charge state distribution and migration time can be altered based on pH of the BGE. Future work will extend this method to incorporate tandem mass spectrometry for online sequence analysis of sulfated GAGs.

Supplementary Material

Refer to Web version on PubMed Central for supplementary material.

Author Manuscript Author Manuscript Author Manuscript Author Manuscript

Acknowledgments

The authors are grateful for generous financial support from the National Institutes of Health (R21HL136271 and P41GM103390). PS would like to acknowledge Jared Lamp (University of Notre Dame) for helpful discussions during manuscript preparation. The authors would like to acknowledge Geert Jan Boons (University of Georgia) and Deirdre Coombe (Curtin University) for previously provided samples utilized in this current study.

References

1. Varki A. Biological roles of glycans. Glycobiology. 2017; 27:3–49. DOI: 10.1093/glycob/cww086 [PubMed: 27558841]
2. Afratis N, Gialeli C, Nikitovic D, Tsegenidis T, Karousou E, Theocharis AD, Pavão MS, Tzanakakis GN, Karamanos NK. Glycosaminoglycans: key players in cancer cell biology and treatment. FEBS Journal. 2012; 279:1177–1197. DOI: 10.1111/j.1742-4658.2012.08529.x [PubMed: 22333131]
3. Barbucci R, Magnani A, Lamponi S, Albanese A. Chemistry and biology of glycosaminoglycans in blood coagulation. Polym Adv Technol. 1996; 7:675–685. DOI: 10.1002/(SICI)1099-1581(199608)7:8<675::AID-PAT609>3.0.CO;2-U
4. Sasisekharan R, Shriver Z, Venkataraman G, Narayanasami U. Roles of heparan-sulphate glycosaminoglycans in cancer. Nat Rev Cancer. 2002; 2:521.doi: 10.1038/nrc842 [PubMed: 12094238]
5. Varki A, Cummings R, Esko J, Freeze H, Hart G, Marth J. Essentials of glycobiology. 1998
6. Xiao Z, Zhao W, Yang B, Zhang Z, Guan H, Linhardt RJ. Heparinase 1 selectivity for the 3,6-di-O-sulfo-2-deoxy-2-sulfamido-α-D-glucopyranose (1,4) 2-O-sulfo-α-L-idopyranosyluronic acid (GlcNS3S6S-IdoA2S) linkages. Glycobiology. 2011; 21:13–22. DOI: 10.1093/glycob/cwq123 [PubMed: 20729345]
7. Wolff JJ, Laremore TN, Busch AM, Linhardt RJ, Amster IJ. Electron detachment dissociation of dermatan sulfate oligosaccharides. J Am Soc Mass Spectrom. 2008; 19:294–304. DOI: 10.1016/j.jasms.2007.10.007 [PubMed: 18055211]
8. Wolff JJ, Amster IJ, Chi L, Linhardt RJ. Electron detachment dissociation of glycosaminoglycan tetrasaccharides. J Am Soc Mass Spectrom. 2007; 18:234–244. DOI: 10.1016/j.jasms.2006.09.020 [PubMed: 17074503]
9. Leach FE 3rd, Wolff JJ, Xiao Z, Ly M, Laremore TN, Arungundram S, Al-Mafraji K, Venot A, Boons GJ, Linhardt RJ, Amster IJ. Negative electron transfer dissociation Fourier transform mass spectrometry of glycosaminoglycan carbohydrates. Eur J Mass Spectrom. 2011; 17:167–176. DOI: 10.1255/ejms.1120
10. Laremore TN, Leach FE, Solakyildirim K, Amster IJ, Linhardt RJ. Glycosaminoglycan characterization by electrospray ionization mass spectrometry including Fourier transform mass spectrometry. Methods Enzymol. 2010; 478:79–108. DOI: 10.1016/s0076-6879(10)78003-4 [PubMed: 20816475]
11. Bielik AM, Zaia J. Multistage tandem mass spectrometry of chondroitin sulfate and dermatan sulfate. Int J Mass Spectrom. 2011; 305:131–137. DOI: 10.1016/j.ijms.2010.10.017 [PubMed: 21860601]
12. Zaia J. Compositional analysis of glycosaminoglycans by electrospray mass spectrometry. Anal Chem. 2001; 73:233–239. DOI: 10.1021/ac000777a [PubMed: 11199971]
13. Zaia J. Tandem mass spectrometry of sulfated heparin-like glycosaminoglycan oligosaccharides. Anal Chem. 2003; 75:2445.doi: 10.1021/ac0263418 [PubMed: 12918989]
14. Li G, Steppich J, Wang Z, Sun Y, Xue C, Linhardt RJ, Li L. Bottom-up low molecular weight heparin analysis using liquid chromatography-Fourier transform mass spectrometry for extensive characterization. Anal Chem. 2014; 86:6626–6632. DOI: 10.1021/ac501301v [PubMed: 24905078]
15. Ly M, Leach FE, Laremore TN, Toida T, Amster IJ, Linhardt RJ. The proteoglycan bikunin has a defined sequence. Nat Chem Biol. 2011; 7:827–833. DOI: 10.1038/nchembio.673 [PubMed: 21983600]

Author Manuscript Author Manuscript Author Manuscript Author Manuscript

16. Li L, Zhang F, Zaia J, Linhardt RJ. Top-down approach for the direct characterization of low molecular weight heparins using LC-FT-MS. Anal Chem. 2012; 84:8822–8829. DOI: 10.1021/ac302232c [PubMed: 22985071]
17. Chi L, Amster J, Linhardt RJ. Mass Spectrometry for the Analysis of Highly Charged Sulfated Carbohydrates. Anal Chem. 2005; 1:223–240. DOI: 10.2174/157341105774573929
18. Laremore TN, Zhang F, Dordick JS, Liu J, Linhardt RJ. Recent progress and applications in glycosaminoglycan and heparin research. Curr Opin Chem Biol. 2009; 13:633–640. DOI: 10.1016/j.cbpa.2009.08.017 [PubMed: 19781979]
19. Zaia J. On-line separations combined with MS for analysis of glycosaminoglycans. Mass Spectrom Rev. 2009; 28:254–272. DOI: 10.1002/mas.20200 [PubMed: 18956477]
20. Volpi N, Galeotti F, Yang B, Linhardt RJ. Analysis of glycosaminoglycan-derived, precolumn 2-aminoacridone–labeled disaccharides with LC-fluorescence and LC-MS detection. Nat Protoc. 2014; 9:541–558. DOI: 10.1038/nprot.2014.026 [PubMed: 24504479]
21. Huang Y, Shi X, Yu X, Leymarie N, Staples GO, Yin H, Killeen K, Zaia J. Improved liquid chromatography-MS/MS of heparan sulfate oligosaccharides via chip-based pulsed makeup flow. Anal Chem. 2011; 83:8222–8229. DOI: 10.1021/ac201964n [PubMed: 21923145]
22. Huang R, Liu J, Sharp JS. An approach for separation and complete structural sequencing of heparin/heparan sulfate-like oligosaccharides. Anal Chem. 2013; 85:5787–5795. DOI: 10.1021/ac400439a [PubMed: 23659663]
23. Zaia J, Khatri K, Klein J, Shao C, Sheng Y, Viner R. Complete molecular weight profiling of low-molecular weight heparins using size exclusion chromatography-ion suppressor-high-resolution mass spectrometry. Anal Chem. 2016; 88:10654–10660. DOI: 10.1021/acs.analchem.6b03081 [PubMed: 27709905]
24. Gill VL, Aich U, Rao S, Pohl C, Zaia J. Disaccharide analysis of glycosaminoglycans using hydrophilic interaction chromatography and mass spectrometry. Anal Chem. 2013; 85:1138–1145. DOI: 10.1021/ac3030448 [PubMed: 23234263]
25. Buszewski B, Noga S. Hydrophilic interaction liquid chromatography (HILIC)—a powerful separation technique. Anal Bioanal Chem. 2012; 402:231–247. DOI: 10.1007/s00216-011-5308-5 [PubMed: 21879300]
26. Pereira L. Porous graphitic carbon as a stationary phase in HPLC: theory and applications. J Liq Chromatogr Relat Technol. 2008; 31:1687–1731. DOI: 10.1080/10826070802126429
27. Ruhaak LR, Deelder AM, Wuhrer M. Oligosaccharide analysis by graphitized carbon liquid chromatography-mass spectrometry. Anal Bioanal Chem. 2009; 394:163–174. DOI: 10.1007/s00216-009-2664-5 [PubMed: 19247642]
28. Karlsson NG, Schulz BL, Packer NH, Whitelock JM. Use of graphitised carbon negative ion LC–MS to analyse enzymatically digested glycosaminoglycans. J Chromatogr B. 2005; 824:139–147. DOI: 10.1016/j.jchromb.2005.07.014
29. Durney BC, Crihfield CL, Holland LA. Capillary electrophoresis applied to DNA: determining and harnessing sequence and structure to advance bioanalyses (2009–2014). Anal Bioanal Chem. 2015; 407:6923–6938. DOI: 10.1007/s00216-015-8703-5 [PubMed: 25935677]
30. Soga T, Igarashi K, Ito C, Mizobuchi K, Zimmermann H-P, Tomita M. Metabolomic profiling of anionic metabolites by capillary electrophoresis mass spectrometry. Anal Chem. 2009; 81:6165–6174. DOI: 10.1021/ac900675k [PubMed: 19522513]
31. Hirayama A, Wakayama M, Soga T. Metabolome analysis based on capillary electrophoresis-mass spectrometry. Trends Anal Chem. 2014; 61:215–222. DOI: 10.1016/j.trac.2014.05.005
32. Karabiber F, McGinnis JL, Favorov OV, Weeks KM. QuShape: Rapid, accurate, and best-practices quantification of nucleic acid probing information, resolved by capillary electrophoresis. RNA. 2013; 19:63–73. DOI: 10.1261/rna.036327.112 [PubMed: 23188808]
33. Heller C, Slater GW, Mayer P, Dovichi N, Pinto D, Viovy J-L, Drouin G. Free-solution electrophoresis of DNA. J Chromatogr A. 1998; 806:113–121. DOI: 10.1016/S0021-9673(97)00656-0
34. Prabhakar V, Capila I, Sasisekharan R. The structural elucidation of glycosaminoglycans. Methods Mol Biol. 2009; 534:147–156. DOI: 10.1007/978-1-59745-022-5_11 [PubMed: 19277554]

Author Manuscript Author Manuscript Author Manuscript Author Manuscript

35. Volpi N, Maccari F, Linhardt RJ. Capillary electrophoresis of complex natural polysaccharides. Electrophoresis. 2008; 29:3095–3106. DOI: 10.1002/elps.200800109 [PubMed: 18633943]
36. Campa C, Coslovi A, Flamigni A, Rossi M. Overview on advances in capillary electrophoresis-mass spectrometry of carbohydrates: a tabulated review. Electrophoresis. 2006; 27:2027–2050. DOI: 10.1002/elps.200500960 [PubMed: 16736462]
37. Zamfir AD. Applications of capillary electrophoresis electrospray ionization mass spectrometry in glycosaminoglycan analysis. Electrophoresis. 2016; 37:973–986. DOI: 10.1002/elps.201500461 [PubMed: 26701317]
38. Sun X, Lin L, Liu X, Zhang F, Chi L, Xia Q, Linhardt RJ. Capillary electrophoresis–mass spectrometry for the analysis of heparin oligosaccharides and low molecular weight heparin. Anal Chem. 2016; 88:1937–1943. DOI: 10.1021/acs.analchem.5b04405 [PubMed: 26714061]
39. Ampofo SA, Wang HM, Linhardt RJ. Disaccharide compositional analysis of heparin and heparan sulfate using capillary zone electrophoresis. Anal Biochem. 1991; 199:249–255. DOI: 10.1016/0003-2697(91)90098-E [PubMed: 1812791]
40. Mitropoulou TN, Lamari F, Syrokou A, Hjerpe A, Karamanos NK. Identification of oligomeric domains within dermatan sulfate chains using differential enzymic treatments, derivatization with 2-aminoacridone and capillary electrophoresis. Electrophoresis. 2001; 22:2458–2463. DOI: 10.1002/1522-2683(200107)22:12<2458::AID-ELPS2458>3.0.CO;2-8 [PubMed: 11519950]
41. Toida T, Linhardt RJ. Detection of glycosaminoglycans as a copper (II) complex in capillary electrophoresis. Electrophoresis. 1996; 17:341–346. DOI: 10.1002/elps.1150170209 [PubMed: 8900940]
42. Lin L, Liu X, Zhang F, Chi L, Amster IJ, Leach FE, Xia Q, Linhardt RJ. Analysis of heparin oligosaccharides by capillary electrophoresis–negative-ion electrospray ionization mass spectrometry. Anal Bioanal Chem. 2017; 409:411–420. DOI: 10.1007/s00216-016-9662-1 [PubMed: 27325464]
43. Shintani, H. Handbook of capillary electrophoresis applications. Springer Science & Business Media; 2012.
44. Kuhn, R., Hoffstetter-Kuhn, S. Capillary electrophoresis: principles and practice. Springer Science & Business Media; 2013.
45. Whatley, H. Basic Principles and Modes of Capillary Electrophoresis. Humana Press; Totowa, NJ: 2001.
46. Grossman, PD., Colburn, JC. Capillary electrophoresis: Theory and practice. Academic Press; 2012.
47. Man Y, Lv X, Iqbal J, Jia F, Xiao P, Hasan M, Li Q, Dai R, Geng L, Qing H, Deng Y. Adsorptive BSA coating method for CE to separate basic proteins. Chromatographia. 2013; 76:59–65. DOI: 10.1007/s10337-012-2337-y
48. Chang WW, Hobson C, Bomberger DC, Schneider LV. Rapid separation of protein isoforms by capillary zone electrophoresis with new dynamic coatings. Electrophoresis. 2005; 26:2179–2186. DOI: 10.1002/elps.200410283 [PubMed: 15861468]
49. Singh A, Kett WC, Severin IC, Agyekum I, Duan J, Amster IJ, Proudfoot AEI, Coombe DR, Woods RJ. The interaction of heparin tetrasaccharides with chemokine CCL5 is modulated by sulfation pattern and pH. J Biol Chem. 2015; doi: 10.1074/jbc.M115.655845
50. Arungundram S, Al-Mafraji K, Asong J, Leach FE, Amster IJ, Venot A, Turnbull JE, Boons G-J. Modular synthesis of heparan sulfate oligosaccharides for structure-activity relationship studies. J Am Chem Soc. 2009; 131:17394–17405. DOI: 10.1021/ja907358k [PubMed: 19904943]
51. Sun L, Zhu G, Zhao Y, Yan X, Mou S, Dovichi NJ. Ultrasensitive and Fast Bottom-up Analysis of Femtogram Amounts of Complex Proteome Digests. Angew ChemInt Ed. 2013; 52:13661–13664. DOI: 10.1002/anie.201308139
52. Sun L, Zhu G, Zhang Z, Mou S, Dovichi NJ. Third-generation electrokinetically pumped sheath-flow nanospray interface with improved stability and sensitivity for automated capillary zone electrophoresis–mass spectrometry analysis of complex proteome digests. J Proteome Res. 2015; 14:2312–2321. DOI: 10.1021/acs.jproteome.5b00100 [PubMed: 25786131]

Author Manuscript Author Manuscript Author Manuscript Author Manuscript

53. Zhu M, Lerum MZ, Chen W. How to prepare reproducible, homogeneous, and hydrolytically stable aminosilane-derived layers on silica. Langmuir. 2012; 28:416–423. DOI: 10.1021/la203638g [PubMed: 22128807]

54. Liu X, Xing J, Guan Y, Shan G, Liu H. Synthesis of amino-silane modified superparamagnetic silica supports and their use for protein immobilization. Colloids Surf, A. 2004; 238:127–131. DOI: 10.1016/j.colsurfa.2004.03.004

55. Kneuer C, Sameti M, Haltner EG, Schiestel T, Schirra H, Schmidt H, Lehr C-M. Silica nanoparticles modified with aminosilanes as carriers for plasmid DNA. Int J Pharm. 2000; 196:257–261. DOI: 10.1016/S0378-5173(99)00435-4 [PubMed: 10699731]

56. Kailemia MJ, Park M, Kaplan DA, Venot A, Boons G-J, Li L, Linhardt RJ, Amster IJ. High-field asymmetric-waveform ion mobility spectrometry and electron detachment dissociation of isobaric mixtures of glycosaminoglycans. J Am Soc Mass Spectrom. 2014; 25:258–268. DOI: 10.1007/s13361-013-0771-1 [PubMed: 24254578]

57. Galeotti F, Volpi N. Online reverse phase-high-performance liquid chromatography-fluorescence detection-electrospray ionization-mass spectrometry separation and characterization of heparan sulfate, heparin, and low-molecular weight-heparin disaccharides derivatized with 2-aminoacridone. Anal Chem. 2011; 83:6770–6777. DOI: 10.1021/ac201426e [PubMed: 21780812]

58. Li D, Chi L, Jin L, Xu X, Du X, Ji S, Chi L. Mapping of low molecular weight heparins using reversed phase ion pair liquid chromatography–mass spectrometry. Carbohydr Polym. 2014; 99:339–344. DOI: 10.1016/j.carbpol.2013.08.074 [PubMed: 24274516]

59. Zaia J, Khatri K, Klein J, Shao C, Sheng Y, Viner R. Complete molecular weight profiling of low-molecular weight heparins using size exclusion chromatography-ion suppressor-high-resolution mass spectrometry. Anal Chem. 2016; 88:10654–10660. DOI: 10.1021/acs.analchem.6b03081 [PubMed: 27709905]

60. Sun X, Sheng A, Liu X, Shi F, Jin L, Xie S, Zhang F, Linhardt RJ, Chi L. Comprehensive identification and quantitation of basic building blocks for low-molecular weight heparin. Anal Chem. 2016; 88:7738–7744. DOI: 10.1021/acs.analchem.6b01709 [PubMed: 27388010]

Author Manuscript Author Manuscript Author Manuscript Author Manuscript

Highlights

- Reverse polarity CE-MS enables the analysis of sulfated GAG mixtures.
- Covalent neutral and cation coatings produce fast and reproducible separations.
- The separation of oligosaccharides from tetra- to dodecasaccharides is demonstrated.
- Structures with sulfation position and epimeric structural differences are resolved.
- More than 80 molecular compositions are determined from complex GAG mixture.

Author Manuscript
Author Manuscript
Author Manuscript
Author Manuscript

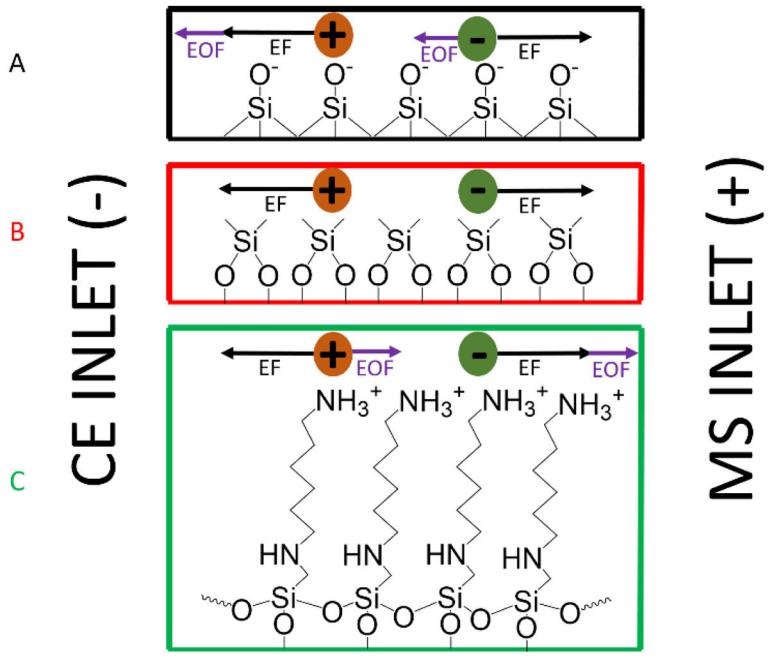

Figure 1.

Diagram depicting the forces of electroosmotic flow (EOF) and electrophoretic forces (EF) that act on analytes during a CZE-MS experiment with three different inner capillary surfaces: (A) Bare fused silica (BFS), (B) DMS coated, and (C) AHS coated.

Author Manuscript Author Manuscript Author Manuscript Author Manuscript

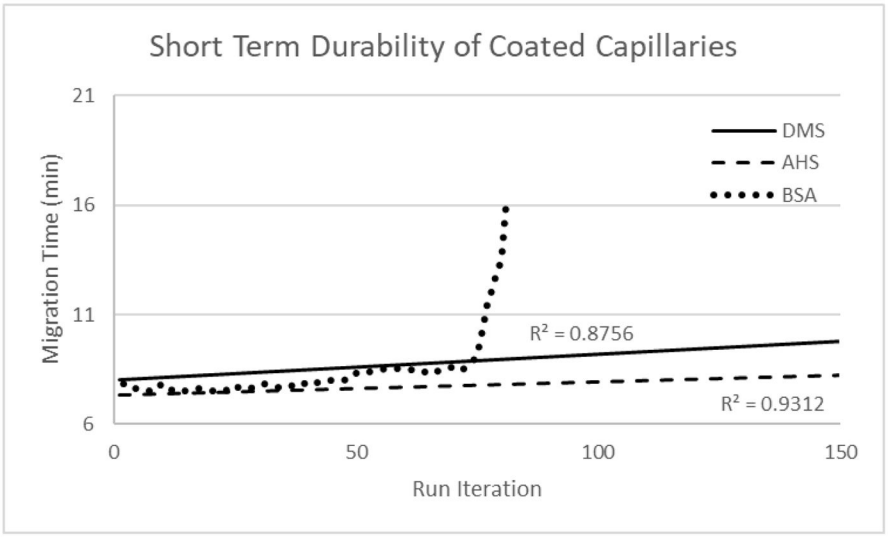

Figure 2.

Short term durability of neutral (DMS, solid line) and cation (AHS, dashed line; BSA, circle dashed line) coated capillaries shown using sample 1 across 150 iterations. The BSA trial was terminated after 81 iterations due to coating failure.

Author Manuscript Author Manuscript Author Manuscript Author Manuscript

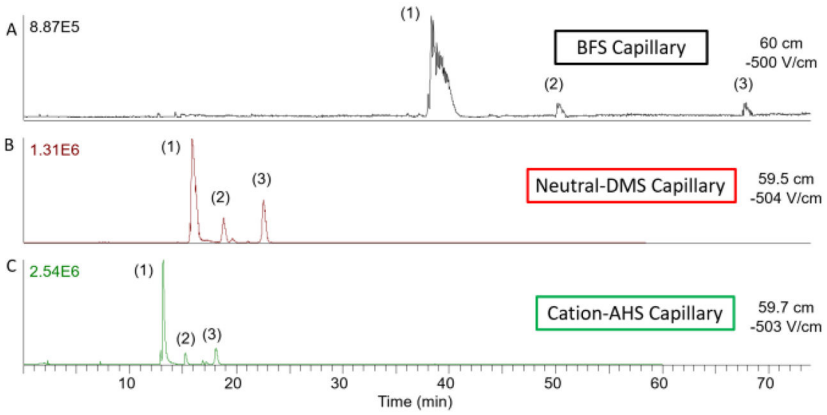

Figure 3.

Electropherogram comparison of migration times based on different capillary coatings. Samples (1), (2), and (3) are tetrasaccharides with different numbers of sulfates. Sample (1) contains six sulfates, (2) has four sulfates, and (3) has three sulfates. Significant improvement in migration time and peak width is observed with neutral (DMS) and cation coated (AHS) capillaries.

Author Manuscript Author Manuscript Author Manuscript Author Manuscript

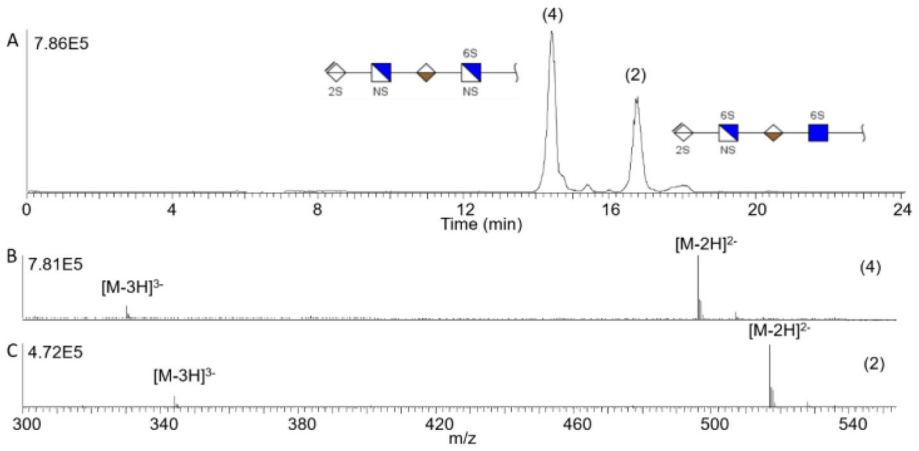

Figure 4.

A) Baseline separation of tetrasaccharide mixture containing samples 4 and 2 with different amino modifications. Mass spectrum of sample 4 (B) and 2 (C) showing the mass difference due to amino modification.

Author Manuscript Author Manuscript Author Manuscript Author Manuscript

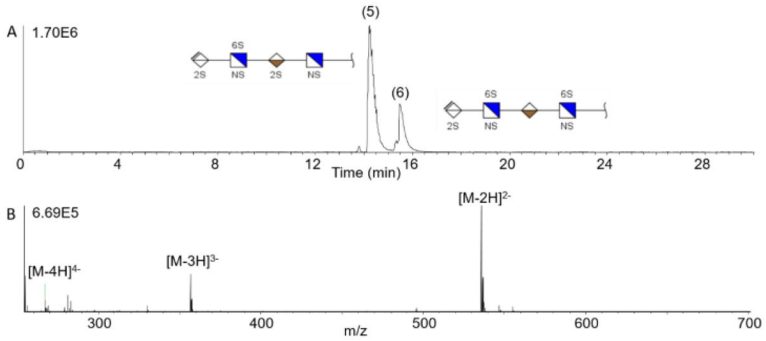

Figure 5.

(A) Baseline CZE separation of a tetrasaccharide mixture on AHS capillary. Sample 5 and 6 are isomers with the same number of sulfate groups and exact mass, but differ in sulfate position on the last two sugar residues. (B) Mass spectrum of sample 5 demonstrating the observed charge state distribution.

Author Manuscript Author Manuscript Author Manuscript Author Manuscript

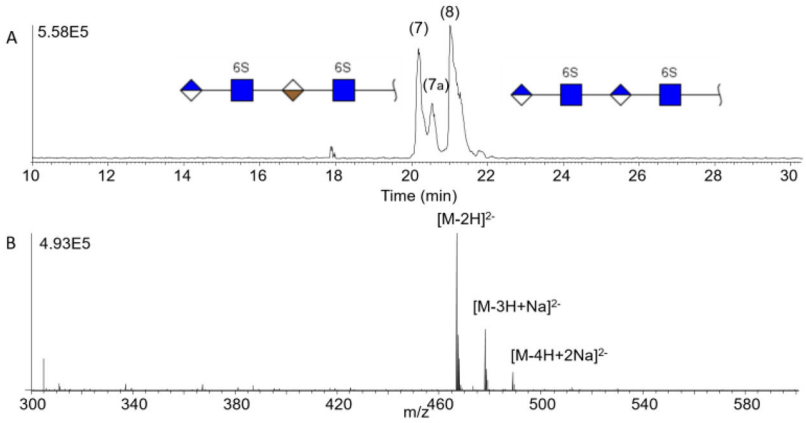

Figure 6.

Baseline separation of a stereoisomer mixture (samples 7 and 8) on AHS capillary. Sample 7 migrates first followed by sample 8. The shoulder peak labeled 7a is attributed to an anomeric form of sample 7.

Author Manuscript Author Manuscript Author Manuscript Author Manuscript

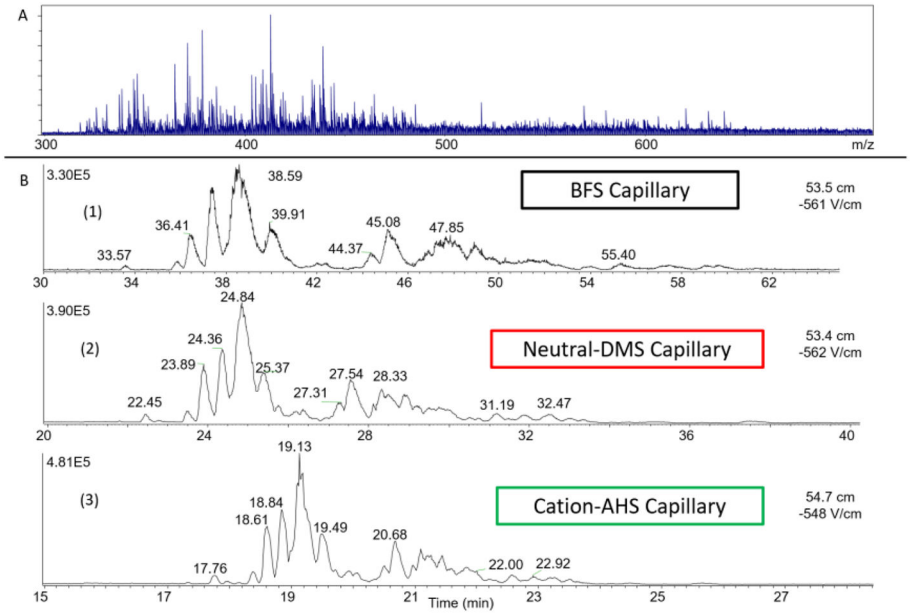

Figure 7.

A) Mass spectrum of Enoxaparin (LMWH) without separation. B) Separation windows of Enoxaparin on uncoated and coated capillaries: (1) BFS (2) DMS, and (3) AHS with migration times decreasing from 1 to 3. The presented migration time window varies between panels 1–3 to enable comparison.

Author Manuscript Author Manuscript Author Manuscript Author Manuscript

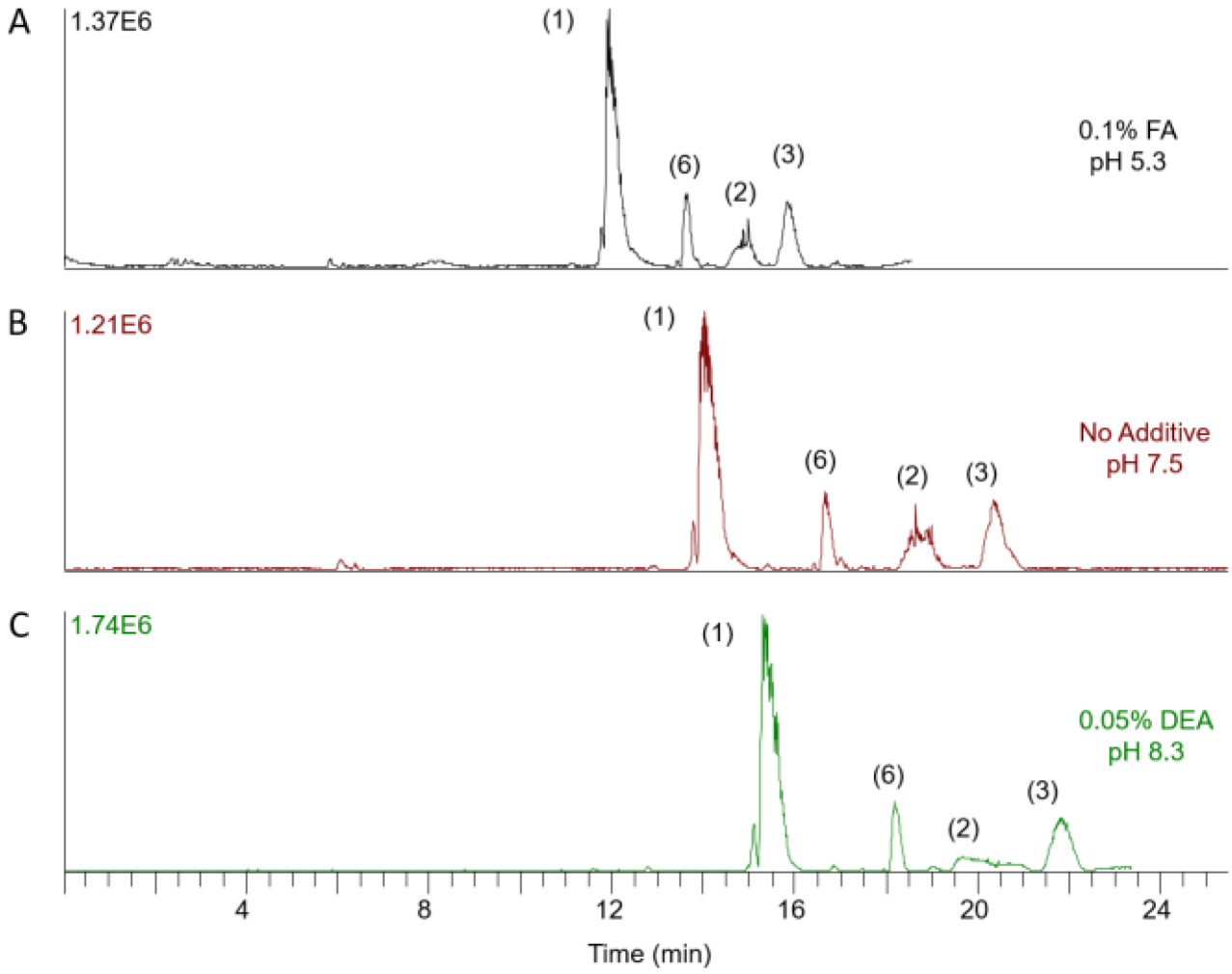

Figure 8.

Effect of additives on four tetrasaccharide standards with an increasing number of sulfates (samples 1–3 and 6) through an AHS coated capillary. The pH of BGE in AHS coated capillaries modulates migration time. Lower pH, from addition of formic acid, leads to faster migration, and higher pH, from diethylamine, leads to slower migration.

Author Manuscript Author Manuscript Author Manuscript Author Manuscript

Table 1

GAG tetrasaccharides used in this study

Tetrasaccharides	Structure Name	Molecular Weight (Da)	Structure
1	ΔUA2S-GlcNS6S-IdoA2S-GlcNS6S	1153.9427	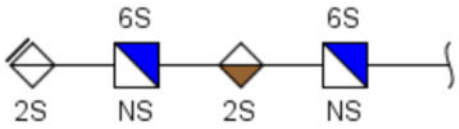
2	ΔUA2S-GlcNS6S-IdoA-GlcNAc6S	1036.0396	
3	ΔUA2S-GlcNS6S-IdoA-GlcNAc	914.0722	
4	ΔUA2S-GlcNS-IdoA-GlcNS6S	994.029	
5	ΔUA2S-GlcNS6S-IdoA2S-GlcNS	1073.9859	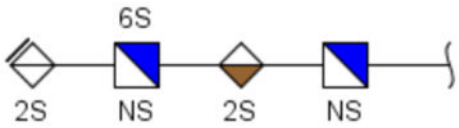
6	ΔUA2S-GlcNS6S-IdoA-GlcNS6S	1073.9859	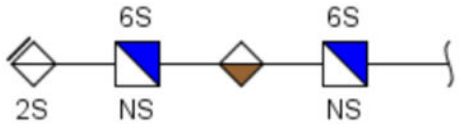
7	GlcA-GlcNAc6S-IdoA-GlcNAc6S	936.1471	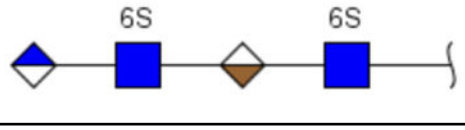
8	GlcA-GlcNAc6S-GlcA-GlcNAc6S	936.1471	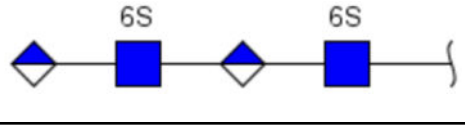

Author Manuscript

Author Manuscript

Author Manuscript

Author Manuscript

Table 2

Effect of BGE Additive on pH

BGE Additive	pH
0.5% FA	4.2
0.4% FA	4.3
0.3% FA	4.6
0.2% FA	4.8
0.1% FA	5.3
None	7.5
0.05% DEA	8.3
0.1% DEA	8.8
0.2% DEA	9.3
0.3% DEA	9.9
0.4% DEA	10.1
BGE: 25 mM ammonium acetate 70% MeOH	